

~~Regime shifted bottom~~**Variations of marine heatwaves and cold spells in the Northwest Atlantic during 1993-2023**

Li Zhai¹, Youyu Lu¹, Haiyan Wang², Gilles Garric³, Simon Van Gennip³

¹Fisheries and Oceans Canada, Bedford Institute of Oceanography, 1 Challenger Dr. Dartmouth, NS, B2Y 4A2, Canada

²Key Laboratory of Marine Hazards Forecasting, National Marine Environmental Forecasting Center, Ministry of Natural Resources, Beijing, China

³Mercator-Ocean International, 2 Av. de l'Aérodrome de Montaudran, 31400 Toulouse, France

Correspondence to: Li Zhai (Li.Zhai@dfo-mpo.gc.ca)

Abstract.

Characteristics of marine heatwaves (MHWs) and cold spells (MCSs) in the Northwest Atlantic during 1993-2023 are derived from a global ocean reanalysis product of the EU Copernicus Marine Service. For ~~the~~ surface parameters, the quantification using the reanalysis data is advantageous [than using the satellite remote sensing data](#) in regions with the presence of seasonal sea ice and strong eddies. At the sea bottom, the reanalysis data well reproduces the observed rising trend and sharp increase of bottom temperature around 2012 on the Scotian Shelf and associated changes of MHW/MCS parameters. The 31 years of reanalysis data enables the quantification of spatial variations, interannual variations and long-term trends of MHW/MCS parameters in the water column ~~for the first time~~ in our study region.

The corresponding parameters of surface MHWs and MCSs are overall similar due to the nearly symmetrical probability distribution of sea surface temperature (SST) anomalies around the mean. On the Scotian Shelf the MHW parameters ~~and temperature~~ present layered structures in the water column, [influenced by the heat flux in the upper layer and the different water mass compositions in the deeper layer](#). ~~In the upper layer from surface to a mid-depth interface, the nearly uniform MHW mean intensity of ~2°C can be mainly attributed to variations of the surface heat flux. From the mid-depth interface to about 130 m depth, the MHW mean intensity has high values of 3–3.5°C due to the combined effects of downward penetration of the upper layer and the lateral advection of water masses. In the deep Emerald Basin below 130 m depth, the MHW intensity has the lowest values of 1.5–2°C. The MHW frequency has relatively uniform values of 1.5–2 per year in the water column, except for low values of less than 1 per year below 130 m depth in the Emerald Basin and below 30 m depth over the Emerald Bank.~~ During 1993-2023, the surface MHW (MCS) total days show increasing (decreasing) trends corresponding to the gradually increasing SST, and the MHW total days reached a peak value of 215 days in 2012 corresponding to the highest annual SST. The bottom temperature shows a stronger increasing trend than the SST, and a ~~sharp increase (regime shift)~~ around 2012, resulting in the increasing (decreasing) trend and regime shift of bottom MHW (MCS) total days. In 2012, the bottom MHW total days experienced a sharp increase and the entire water column was

Commented [LZ1]: I am not sure if we should change the title as suggested by one reviewer because I am not sure that the regime shift occurred in the entire Northwest Atlantic or just Scotian Shelf.

Commented [YL2R1]: Keep the original title.

warmer than the climatology. The opposite condition presented in 1998 with the longest bottom MCS total days of ~300 near the coast. The quantification of the extreme conditions in 2012 and 1998 supports the results of previous studies on the impacts of these conditions on several marine life species.

1 Introduction

Marine heatwaves (MHWs) and marine cold spells (MCSs) are extreme warm and cold events of the ocean water, respectively. MHWs have been observed in all ocean basins (Collins et al., 2019) and ~~have been~~ extensively studied. Globally, MHWs, defined relative to a fixed climatological period, have become more frequent, long-lasting, and intense since the 1980s under global warming (Frölicher et al., 2018; Oliver et al., 2018; Fox-Kemper et al., 2021). Regionally, local processes, large-scale climate modes, and teleconnections also play important roles in MHW occurrences (Holbrook et al., 2019; Sen Gupta et al., 2020; Capotondi et al., 2024). ~~For example, in the Northwest Pacific, interannual variations of surface MHWs are correlated with various large-scale atmosphere-ocean indices including the El Niño index (Wang et al., 2024). On the shelf seas of the Northwest Atlantic, nearly half of the surface MHWs are initiated by the positive heat flux anomaly into the ocean, and advection and mixing are the primary drivers for the decay of most MHWs (Schlegel et al., 2021b). On the Newfoundland and Labrador Shelf, the summer and fall MHWs in 2023 were impacted by stratification, winds, and advection (Soontiens et al., 2025).~~ ~~These connections between surface MHWs and physical drivers, thus identified, can be utilized to predict the occurrence of future MHW events. With these identified physical drivers that trigger and maintain the events, MHWs could persist and induce severe impacts on marine ecosystems. Identifying the physical drivers that trigger and maintain the MHWs (MCSs) is important for understanding and predicting the variations of these events and their impacts on marine ecosystems.~~

Previous studies have revealed the negative impacts of MHWs ~~and MCSs~~ on marine ecosystems. For example, MHWs can cause coral bleaching, destroy kelp forests, and alter the migration patterns of marine species (Santora et al., 2020; Beaudin and Bracco, 2022). MHWs have also affected commercial fisheries in Canadian waters. In the Northeast Pacific, intense and long-lasting heat events, such as “the Blob”, led to fisheries collapses (Free et al., 2023). In Atlantic Canada, extreme heat events affect the physiological behaviour of aquaculture Atlantic Salmon, i.e., the increases of heart rates and decreases of motions (Korus, 2024). ~~Previous studies have revealed the linkage of the declining North Atlantic right whale population was related to the significant warming in the Gulf of Maine and the western Scotian Shelf over the recent decades (Meyer-Gutbrod et al., 2021). and The impacts of the extreme cold (warm) event in 1998 (2012) on certain fishery species have also been studied. In 1998, shortly after the cold Labrador Slope Water replaced the Warm Slope Water, the catches of porbeagle shark and silver hake in the Emerald Basin dramatically declined (Drinkwater et al., 2002). The~~ widespread 2012 warm event in the Northwest Atlantic, ~~with large anomalies throughout significant in~~ the water column and at ~~the~~ sea bottom, had opposite effects on different commercial fisheries. It adversely impacted the snow crab juvenile

stages, resulting in a temporary decrease in snow crab abundance on the western Scotian Shelf (Zisserson and Cook, 2017). In the Gulf of Maine, this warm event caused earlier inshore movement of lobsters in the spring, leading to enhanced lobster growth, an extended fishing season, and record landings (Mills et al., 2013).

Compared with MHWs, there have been fewer studies on MCSs. Globally and regionally, the frequency and intensity of surface MCSs show decreasing trends during 1982-2020 associated with the SST increase (Mohamed et al., 2023; Peal et al., 2023; Schlegel et al., 2021; Wang et al., 2022). Changes in atmospheric forcing, ocean circulation and coastal upwelling can drive local cold events at sea surface (Schlegel et al., 2017) and throughout the water column in shallow coastal bays (Casey et al., 2024).

Studies on surface extreme temperature events commonly use sea surface temperatures (SST) based on satellite remote sensing (e.g., Wang et al., 2022; Peal et al., 2023). Such studies are limited to the upper ocean and ice-free areas, and the analysis results are impacted by the observational noises, and cloud correction and interpolation schemes used to generate various levels of satellite SST products. Subsurface extreme events have been less well studied due to the scarcity of temperature observations below the surface, leading to limited knowledge about whether and how extreme events at depth have changed over the past decades (Collins et al., 2019). Results from high-resolution numerical ocean models, particularly those reanalysis products achieved through data assimilation, have been alternatively used to study the extreme temperature events, both at surface and at bottom (e.g., Amaya et al., 2023a; Wang et al., 2024). The study of Amaya et al. (2023a) revealed stronger and longer MHWs at bottom than at surface in the shelf seas of North America, but it did not quantify the interannual and long-term variations of MHW characteristics.

Motivated by the results of previous studies, in this study we try to quantify the space-time variations of MHWs and MCSs in the Northwest Atlantic, from surface to water column to bottom, with the ultimate goal to better support fisheries in this region. Our study region (Fig. 1a) can be sub-divided into includes five locations: (1) Newfoundland and Labrador Shelf (NLS) to the north of Grand Banks; (2) extending in the north to the Grand Banks; (3) Gulf of St. Lawrence (GSL), a semi-enclosed sea connecting to the NLS and Scotian Shelf (SS); (4) Scotian Shelf, an open, straight and rugged shelf, adjoining the Gulf of Maine in the southwest and Scotian Slope off the shelf; (5) Gulf of Maine and Bay of Fundy, a tidally energetic semi-enclosed sea; and (6) Scotian Slope. The physical oceanography in the region is quite complex, due to the influences of the strong multi-scale variability of atmospheric forcing, river runoff, tides, sea-ice, the strong ocean circulation of the Gulf Stream, North Atlantic Current and Labrador Current, and the meso-scale eddies, etc. (e.g., Loder et al., 1998; Brickman et al., 2018; Ma et al., 2022). The water masses of NLS and Grand Banks are strongly affected by the major circulation features in the study region consist of southward Labrador Current that flowing southward on transports cold and fresher water and sea-ice. The Scotian Slope water is influenced by the mixture of warm eddies shed from the eastward Gulf of Stream/North Atlantic Current and the occasional westward intrusion of the Labrador Current near the tail of Grand Banks. The GSL is influenced by the significant freshwater discharge of rivers including the St. Lawrence River, sea-ice formed locally and transported in from NLS, and inflows from NLS, Grand Banks and Scotian Slope. The SS is influenced by the outflow from the GSL and the intrusion of Scotian Slope water. The Gulf of Maine and Bay of Fundy are

Formatted: English (United States)

97 ~~influenced by the SS and the of Scotian Slope water. the NLS, a cyclonic circulation in the GSL with an outflow onto SS.~~
98 ~~Nova Scotian Current on the inner SS and a shelf break flow on the outer SS (Loder et al., 1998).~~ Our analysis results will be
99 mainly based on the daily data from an ocean reanalysis product, in comparison with analyses of satellite SST and mooring
100 observations. Main results include 1) characteristics of the spatial distributions of MHW and MCS parameters; 2) the
101 linkages between surface and water column extreme events; and 3) interannual variations and long-term trends, and their
102 relationship with temperature variations and the forcing mechanisms.

103 **2 Datasets and analysis methods**

104 **2.1 Datasets**

105 Table 1 lists the datasets analyzed in this study. Product ref. no. 1 is the daily temperature during 1993-2023 from
106 the global ocean eddy-resolving reanalysis with a 1/12° horizontal resolution, referred to as GLORYS12V1 ~~(GLORYS)~~,
107 The GLORYS12V1 temperature data remains continuous in ice-covered regions, which helps to compensate for the
108 limitations of spatial and temporal coverage of satellite observations in those areas.

109 Products ref. no. 2 ~~during 1993-2016~~ and no. 3 ~~during 2017-2023~~ are global ocean SST analysis produced daily on
110 an operational basis at the Canadian Meteorological Centre (CMC). The analysis incorporates *in situ* observations and
111 retrievals from one microwave and three infrared sensors (Brasnett, 2008), ~~referred to as CMC-SST~~. According to the
112 assessment by Fiedler et al. (2019), the CMC ~~SST~~ data show low standard deviations and mean differences to the
113 independent Argo observations, in comparison with other long-term SST analyses including the ESA SST CCI (European
114 Space Agency Sea Surface Temperature Climate Change Initiative) and MyOcean OSTIA (Operational Sea Surface
115 Temperature and Ice Analysis) available from the Copernicus marine catalogues. Product ref. no. 3 at 0.1° resolution during
116 2017-2023 is linearly interpolated onto the 0.2° grids of product ref. no. 2, thus creating a dataset on unified grids covering
117 1993-2023. CMC-SST has no values at locations and time when sea ice is present.

118 Product ref. no. 4 is the observed daily bottom temperature since 2008 from a bottom-mounted mooring at a
119 location on the inner Scotian Shelf with a water depth of 160 m (Fig. ~~ure~~ 1, location 1), from the Atlantic Zone Monitoring
120 Program (AZMP) of Fisheries and Oceans Canada. The mooring is situated on the path of the coastal Nova Scotia Current
121 (Hebert et al., 2023). The mooring is ~~repositioned-redeployed~~ annually in the fall AZMP survey, ~~hence-and~~ the data is only
122 available until September 2023 for this study.

123

Product Ref. erence -No. & Abbreviation	Product ID & type	Data access	Documentation
1: GLORYS12v1	GLOBAL_MULTIYEAR_PHY_001_030, numerical models	EU Copernicus Marine Service Product (2023) https://doi.org/10.48670/moi-	Product User Manual (PUM): Dré villon et al., 2023a Quality Information Document (QUID): Dré villon et al., 2023b

Formatted Table

124
125

		00021	Journal article: Lellouche et al., 2021
2: CMC-SST	GHRSSST Level 4 CMC 0.2 deg global sea surface temperature analysis, 1993-2016	https://doi.org/10.5067/GHC-MC-4FM02	Journal article: Brasnett, 2008; CMC 2012
3: CMC-SST	GHRSSST Level 4 CMC 0.1 deg global sea surface temperature analysis, 2017-2023	https://doi.org/10.5067/GHC-MC-4FM03	Journal article: Meissner et al., 2016; CMC 2016
4: mooring data	Mooring bottom temperature at ~ 160 m from the AZMP	https://www.dfo-mpo.gc.ca/science/data-donnees/azmp-pmza/index-eng.html	Hebert et al., 2023

Table 1: Product reference table.

126

2.2 Definition and quantification of marine heatwaves and cold spells

126

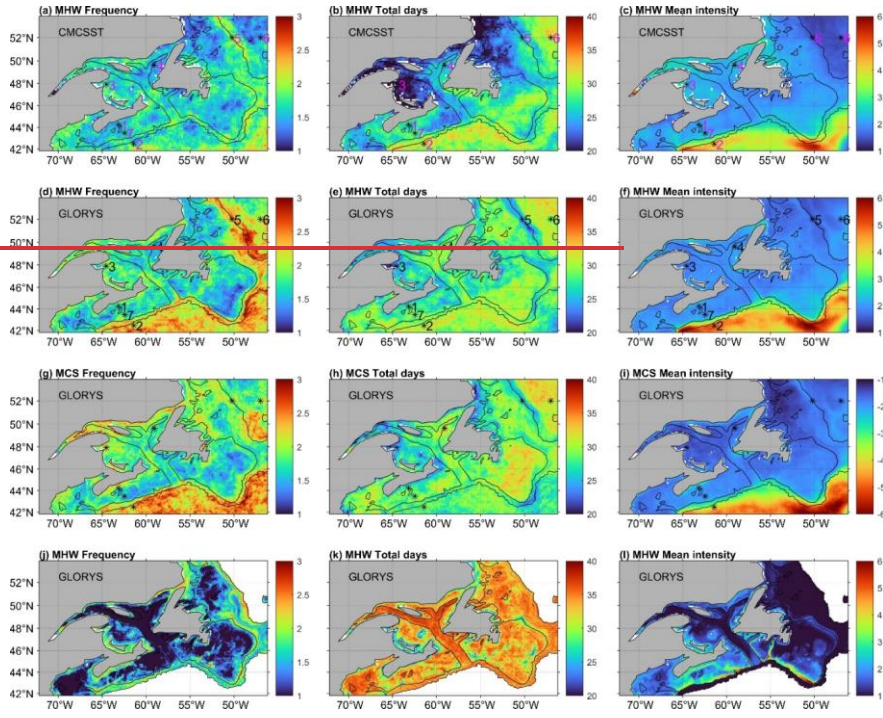
127 Following Hobday et al. (2016), the MHWs (~~MCSs~~) are defined as periods of extremely warm (~~cold~~) water that last
128 continuously for five or more days. ~~Schlegel et al. (2017) defined the MCS are defined similarly as anomalously cold water~~
129 ~~events following Schlegel et al. (2017). similar to the MHW definition by Hobday et al. (2016).~~ We use the SST data to
130 compute the surface MHW and MCS parameters, and the temperature at ocean floor to compute the bottom MHW and MCS
131 parameters. A seasonally varying climatological percentile threshold method is used to detect MHWs (MCSs). ~~No~~
132 ~~detrending is applied to the temperature data prior to the MHW/MCS analysis because we want to maintain the consistency~~
133 ~~and be able to compare with the results of other MHW/MCS studies in the Northwest Atlantic (Galbraith et al., 2023;~~
134 ~~Soontiens et al., 2025), and to emphasize the effects of ocean warming on the changing characteristics of MHWs/MCSs.~~
135 The climatological mean and thresholds (90th and 10th percentiles of data values) are calculated for each day of the year with
136 all data from multiple years within an 11-day window centred on that day. The climatology and thresholds are defined over
137 30 years from 1993 to 2022 for GLORYS [12V1](#) and CMC-SST, and from 2010 to 2022 for the mooring ~~observations data~~. A
138 30-day ‘moving window’ is applied to smooth the daily climatology. The MHWs and MCSs are defined for temperatures
139 above the 90th and below the 10th percentile values, respectively. Events that occur less than 2 days apart ~~are will be~~
140 considered as one continuous event. The statistics for each MHW (MCS) event are calculated using a Matlab-based tool
141 (Zhao and Marin, 2019). This study ~~is going to will~~ focus on the annual statistics of frequency, total days and mean intensity.
142 Frequency refers to the total count of MHW (or MCS) events in each year, while total days are the total number of MHW (or
143 MCS) days in each year. ~~The MHW (or MCS) duration is roughly the total days divided by the frequency. The duration of~~
144 ~~each MHW (MCS) event is defined as the period over which the temperature is greater (lower) than the seasonally varying~~
145 ~~threshold value. The mean intensity of each event is the mean SST anomaly during one that event. The mean intensity is the~~
146 ~~average of the intensities of events during that year. In this study we use SST data to computer surface MHWs and MCSs~~
147 ~~parameters, and the temperature at ocean floor to compute bottom MHWs and MCSs parameters.~~

148 3 Results

149 3.1 Spatial distribution of annual surface MHW and MCS parameters

150 For surface M~~W~~H~~W~~s, GLORYS12V1 and CMC-SST data (Figs. 1c-f) ~~obtain overall similar magnitudes and~~
151 spatial patterns of ~~frequency, total days and~~ mean intensity (Figs. 1a-f), ~~but show distributions different magnitudes of~~
152 ~~frequency in deep waters and total days in the seasonally ice-covered areas.~~ For frequency (Figs. 1a and d), ~~both data obtain~~
153 values of 1-2 ~~events~~ per year on ~~the shelf.~~ ~~are lower than 2-3 in deep regions beyond the shelf break. and in~~ deep regions
154 ~~(near and beyond the 2000 m isobath) with water depth greater than 2000 m.~~ GLORYS12V1 and CMC-SST obtains higher
155 ~~and lower than 2.5 events per year, respectively. frequency MHWs than CMC-SST.~~ For the total days (Figs. 1b and e),
156 GLORYS12V1 and CMC-SST obtain similar values greater than 30 days per year beyond ~~the~~ shelf break on the Scotian
157 Slope and to the east of ~~the~~ Labrador Shelf, and over the Grand Banks ~~offer Newfoundland (GBN).~~ ~~Ove the Newfoundland~~
158 ~~and Labrador Shelf and in the southern and western Gulf of St. Lawrence where the seasonal sea-ice coverage exists. In the~~
159 ~~Gulf of Maine, eastern Scotian Shelf, Gulf of St. Lawrence and Labrador Shelf.~~ GLORYS12V1 obtains 25-30 days, higher
160 than ~~about 20-25~~ days from CMC-SST. ~~In the Gulf of Maine, eastern Scotian Shelf and eastern Gulf of St. Lawrence,~~
161 ~~GLORYS12V1 obtains 25-30 days while CMC-SST obtains 20-25 days.~~ For the mean intensity (Figs. 1c and f), both
162 GLORYS12V1 and CMC-SST obtain consistently higher values of 3-6°C in the deep water of ~~the~~ Scotian Slope and to the
163 east of ~~the~~ southern G~~B~~rand Banks~~N~~, and lower values of less than 2.5°C on the shelf and in the deep water to the east of ~~the~~
164 Labrador Shelf. ~~The MHW parameters derived from GLORYS12V1 are consistent with those based on the thermograph~~
165 ~~network daily mean temperatures in the Gulf of St. Lawrence using the 1991-2020 reference period (Galbraith et al., 2023).~~

166



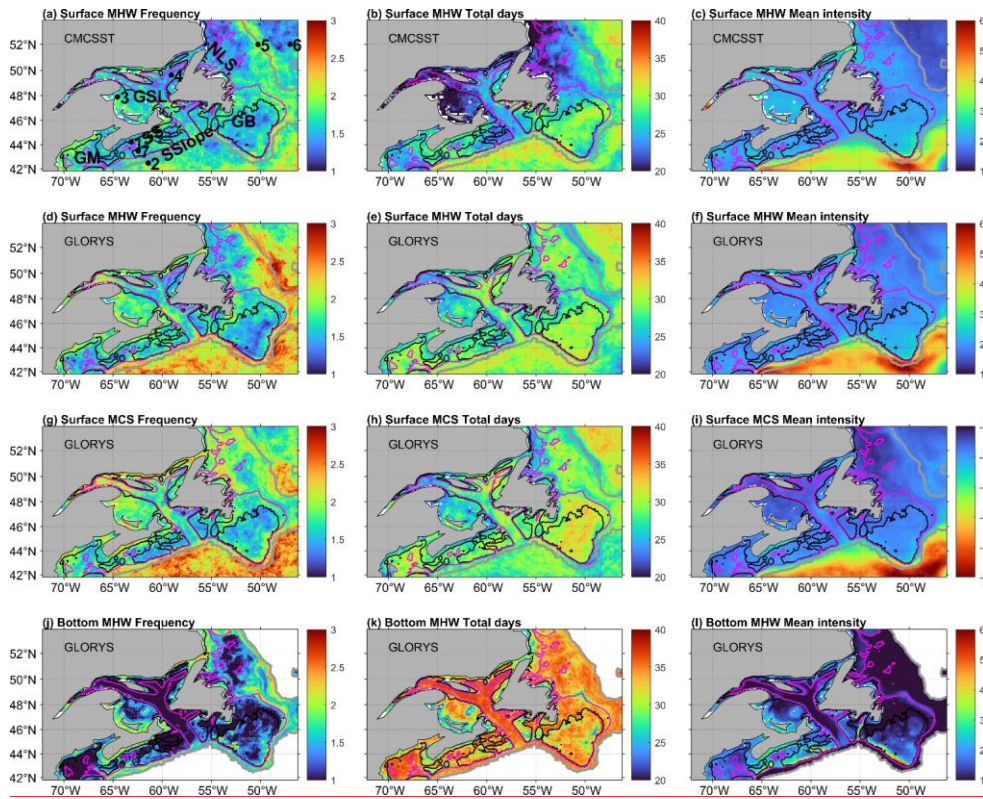
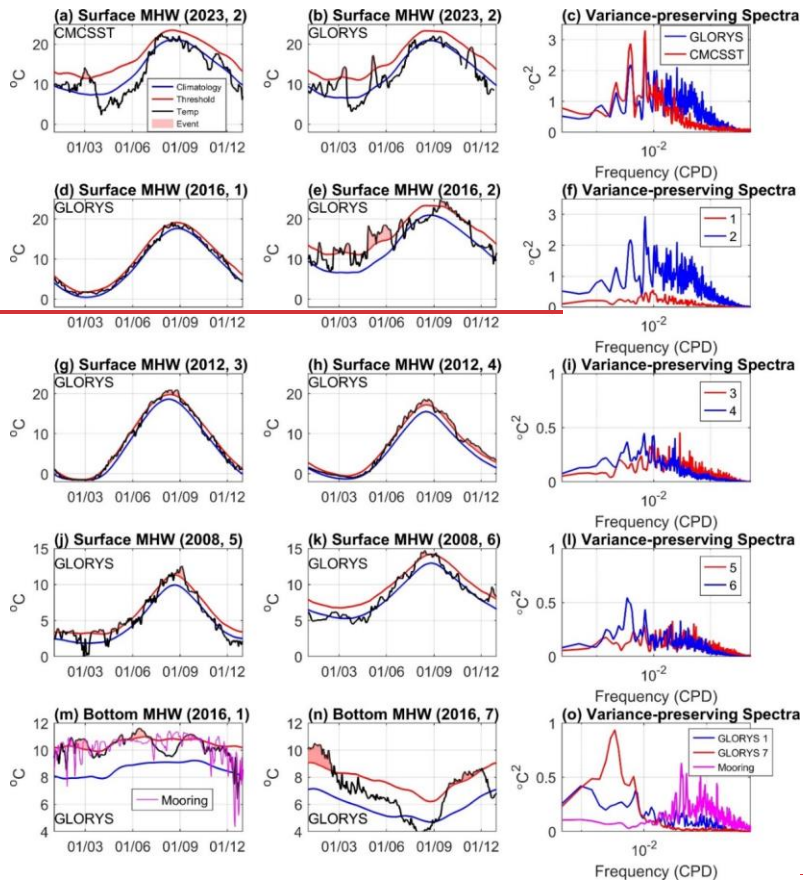


Figure 1: Mean of surface MHW (a-f) and MCS (g-i) characteristics during 1993-2022 derived from (a-c) CMC-SST and (d-i) GLORYS^{12V1}. (j-l) Mean of bottom MHW characteristics during 1993-2022 derived from GLORYS. From left to right: frequency (unit in number of events per year), total days (unit in days per year), and mean intensity (unit in °C). The 100, 200 and 2000 m isobaths are represented by black, magenta and grey lines respectively. Panel (a): Stations 1-7 indicated by the asterisks-solid circles in panel (a) are selected to examine the time series of MHW/MCS characteristics, located at longitude/latitudes of [redacted]. The Halifax line is the line between stations 1 and 2. Abbreviations: GB, Grand Banks; GM, Gulf of Maine; GSL, Gulf of St. Lawrence; NLS, Newfoundland and Labrador Shelf; SS, Scotian Shelf; SSlope, Scotian Slope; CB, Cabot Strait.

Commented [LY3]: Add lat/lon values here



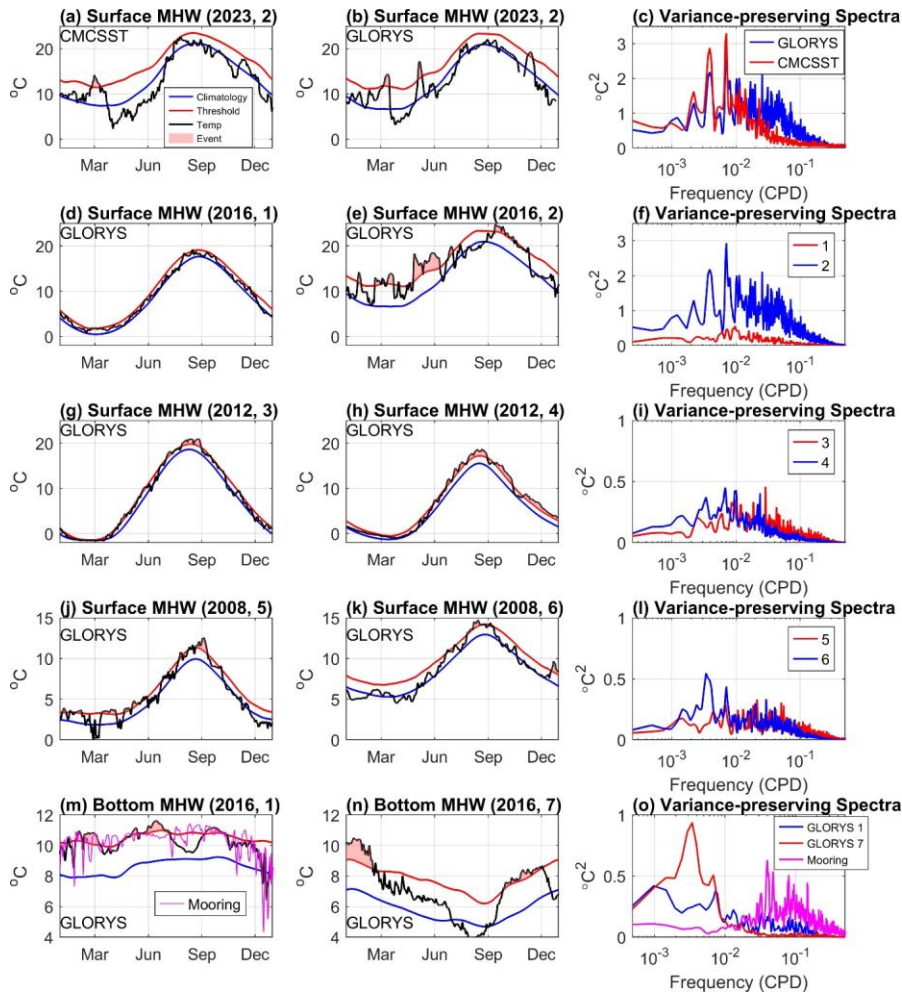


Figure 2: Left and middle columns: Time series of sea temperature Evolution of and detection of MHW in selected years at the surface (a-e, g-i, j-k) and at the seabed (m-n) at 7 locations marked in Figure 1a. The numbers in the bracket indicate the year and location. Right column: Variance preserving spectra of (c, f, i, l) surface temperature for the period of during 1993-2022 and (o) bottom temperature during for the period of 2010-2022.

184 The causes of the differences in the MHW parameters derived from GLORYS12V, CMC-SST and mooring data,
185 and the spatial distributions derived from GLORYS12V1, are explored through examining the time series of sea
186 temperatures and the detection of MHWs at selected location (denoted in Fig. 1a) in selected years, and the variance-
187 preserving spectra during 1993-2022 shown in Fig. 2. The selection of years is based on annual time series of the MHW
188 parameters at these locations (not shown), ensuring that the differences in the MHW parameters between the left and middle
189 columns are consistent with the 1993-2022 averaged statistics shown in Fig. 1. First, on the Scotian Slope (The differences
190 between GLORYS and CMC-SST in the higher surface MHW frequency from GLORYS12V1 than from CMC-SST and
191 total days on the Scotian Slope can be explained by their differences in the SST time series (Figs. 2a-b) and variance-
192 preserving spectra of the SST time series during 1993-2022 at location 2 (Fig. 2c) at location 2 denoted in Fig. 4. Compared
193 with CMC-SST, GLORYS12V1 obtains-achieves more frequent and stronger temperature variations, and higher spectral
194 power at time scales less-shorter than 50 days. For instance, in the selected year 2023, GLORYS12V1 shows the more
195 frequent and stronger SST variations, and detected three shorter MHW events whereas CMC-SST detected one longer
196 MHW event (Figs. 2a-b). Note that the high-frequency SST variations in the CMC-SST are impacted by the cloud correction
197 and interpolation schemes applied to the original satellite data in generating the CMC-SST product.

198 In the southern and western Gulf of St Lawrence, the St. Lawrence Estuary, and on the Labrador and Newfoundland
199 Shelf, CMC-SST obtains-has shorter total days than GLORYS12V1 (Figs. 1b and e). This can be attributed to the missing
200 data in CMC-SST due to the presence of sea ice in these regions. In the selected year 2011, Fig. 3A presents We plotted the
201 SST time series at a location (52.8°N, 55.2°W) on the Labrador Shelf, and performed one additional analysis to help explain
202 the difference. Figures A3 The original CMC-SST data has a significant number of missing values -a and b show that surface
203 MHWs from January to April during the presence of seasonal sea-ice (Fig. A3a), leading to the 90th threshold above of that
204 derived from GLORYS12V1 (Figs. A3a and b). 2011 derived from CMC-SST occur less frequently and have shorter
205 durations than those of GLORYS. To help illustrate these differences, we filled If the missing values of the original CMC-
206 SST are filled of CMC-SST with a freezing temperature of -1.8 °C, the resulting 90th threshold (Fig. A3c) and the total days
207 of the detected MHWs are closer to that derived from GLORYS12V1 (Figs. A3 b). Thus, the shorter MHW total days from
208 CMC-SST in regions with the presence of seasonal sea-ice are due the biased 90th threshold caused by the missing SST data
209 values and then calculated the MHW parameters shown in Figure A3 c. Comparing Figures A3 a and c, we find that the
210 MHW event in January lasts longer and two more MHW events are detected after the missing data are filled because the
211 90th threshold in CMC-SST with no missing values is shifted to a lower value. Figure A3 c is consistent with Figure A3 b,
212 suggesting that the difference in MHW parameters in ice-covered areas such as the Gulf of St. Lawrence, Labrador and
213 Newfoundland shelf and eastern Scotian Shelf is caused by threshold changes with and without missing data.

214 The spatial patterns of surface MHW parameters from GLORYS12V1 (Figs. 1d-f) are explained next. The
215 differences between the shelf and the Scotian Slope are demonstrated by comparing the SST time series in 2016 and spectra
216 at locations 1 and 2 (Figs. 2d-f). At all the time scales, location 2 shows much stronger SST variability because it is located
217 in the Scotian Slope water, which where the water mass is affected by a succession of warm and cold oscillations and eddies.

Formatted: Superscript

Formatted: Superscript

Formatted: Superscript

For example, in the selected year 2016, GLORYS12V1 detected 6 strong MHW events at location 2 while only one weak event at location 1. In the Gulf of St. Lawrence, the average annual frequency (Fig. 1d) is lower in the northeastern (location 4) and higher in the southwestern parts (location 3) regions, while the total days (Fig. 1e) show the opposite pattern. This is consistent with At locations 3 and 4, the SST time series in the selected year 2012 are similar (Figs. 2g-h), and the variance preserving spectra (Fig. 2i). That is, the spectral energy (Fig. 2i) at location 3 is higher at time scales shorter than 100 days hence leading to higher MHW frequency, and at location 4 is higher at time scales longer than 100 days hence leading to longer durations. The higher total days at station 4 in 2012 are due to the long durations of warming above climatology in fall and winter. Off the Labrador Shelf, over a narrow zone near the 2000 m isobath (location 5), the surface MHW frequency is higher while the total days are shorter, compared to shelf water to the west and the deep water to the east (location 6). This again can be explained by the stronger SST variability at time scales shorter than 100 days at location 5 and longer than 100 days at location 6, respectively (Figs. 2j-l). Location 5 is along the path of the offshore Labrador Current, where the SST anomalies and seasonal cycle are both strong, which can be attributed to the variations of the temperature front in this area (e.g., Lu et al., 2006).

For the surface MCSs derived from GLORYS12V1, their frequency, total days and mean intensity (Figs. 1g-i) show similar magnitudes and spatial distribution with those of surface MHWs (Figs. 1d-f). The MCS parameters derived from CMC-SST (not shown) is also similar with the surface MHW parameters derived from GLORYS12V1 (Figs. 1a-c). Differences between the MCS and MHW parameters derived from GLORYS12V1 are evident in some areas, e.g., on the Scotian Slope (near location 2) the MHWs have lower frequency and higher mean intensity than the MCSs. These similarities and differences can be explained by the probability distribution of SST anomalies at representative sites shown in Fig. A1. The normalized histograms are nearly symmetrical around the mean, with equal median and mean values. At location 2 the median value is less than the mean, suggesting a positive skewness of SST anomalies on the Scotian Slope due to the dominance of warm-core eddies at the poleward side of the Gulf Stream (e.g., Thompson and Demirov, 2006). Such asymmetric distribution of SST anomalies corresponds to stronger MHWs than MCSs (Schlegel et al., 2021a; Wang et al., 2022).

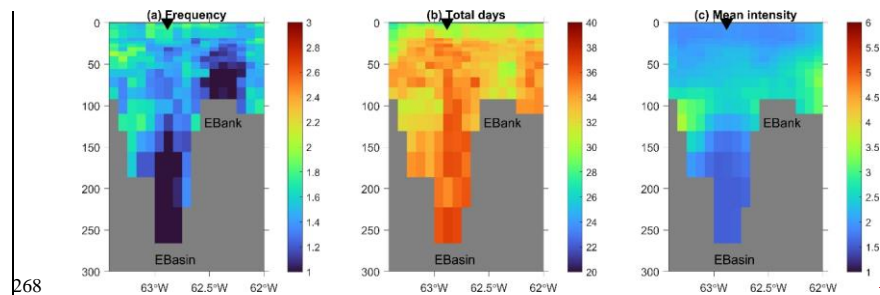
3.2 Distribution of MHW parameters over the sea floor and in the water column

The frequency, total days and mean intensity of bottom MHWs on the shelf derived from GLORYS12V1 (Figs. 1j-l) show different magnitudes and spatial distributions compared to surface MHWs. Our findings are consistent with Amaya et al. (2023a) who showed that bottom MHW intensity and duration vary strongly with bottom depth. The bottom MHW frequency (Fig. 1j) shows fewer events (< 1 per year) in deep basins and channels, and more events (2–3 per year) along the coast and shelf break. The bottom MHW total days (Fig. 1k) exhibit weak spatial variations across the entire region with values of 30–35 days per year, and larger values in deeper basins and channels than in shallow waters. This implies that the bottom MHW durations (roughly total days divided by frequency) are longer in deep basins and channels than in shallow

251 water. The bottom MHWs intensity (Fig. 1l) ranges from 1°C in deeper parts of the continental shelves to 6°C along the
 252 edges of the Scotian Shelf and southern ~~GBN-Grand Banks~~, where water intrusions from the shelf break occur.

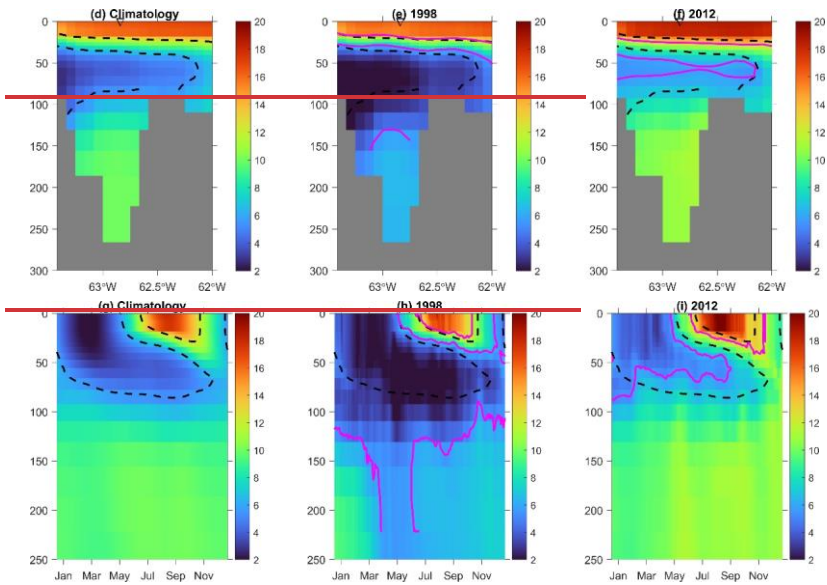
253 We selected two locations on the Scotian Shelf (~~locations 1 and 7~~) to illustrate the difference in MCS characteristics
 254 at the sea floor (Figs. 2m-o). Location 1 is the mooring site near the coast where the water depth is 160 m, and location 7 is
 255 on the Emerald Bank in the middle of the Scotian Shelf where the water depth is 66 m. At location 1, both GLORYS12V1
 256 and mooring ~~data~~observations (Fig. 2m) show that bottom temperatures in 2016 were generally above the mean climatology
 257 and extreme heat events ~~awere~~ detected throughout the year. However, mooring data shows some intense cold spikes that are
 258 not captured by GLORYS12V1 (Fig. 2m). Correspondingly, compared with the mooring data, the spectral energy of
 259 GLORYS12V1 is lower at time scales shorter than 100 days and higher ~~energy~~ at longer than 100 days (Fig. 2o). At location
 260 7, GLORYS detected ~~esd~~ two MHW events with longer durations in 2016 (Fig. 2n). The power spectra ~~of two locations~~ (Fig.
 261 2o) –show that location 1 has more energy at time scales ~~lower-shorter~~ than 100 days, corresponding to higher MHW
 262 frequency and mean intensity, while location 7 shows stronger variability at time scales longer than 100 days, corresponding
 263 to longer MHW duration and lower intensity. The strong variations of bottom temperature at shorter than 100 days at
 264 location 1 are likely related to the strong fluctuations of the coastal Nova Scotia Current driven by local winds at synoptic
 265 scales (Dever et al., 2016).

266
 267



269

270



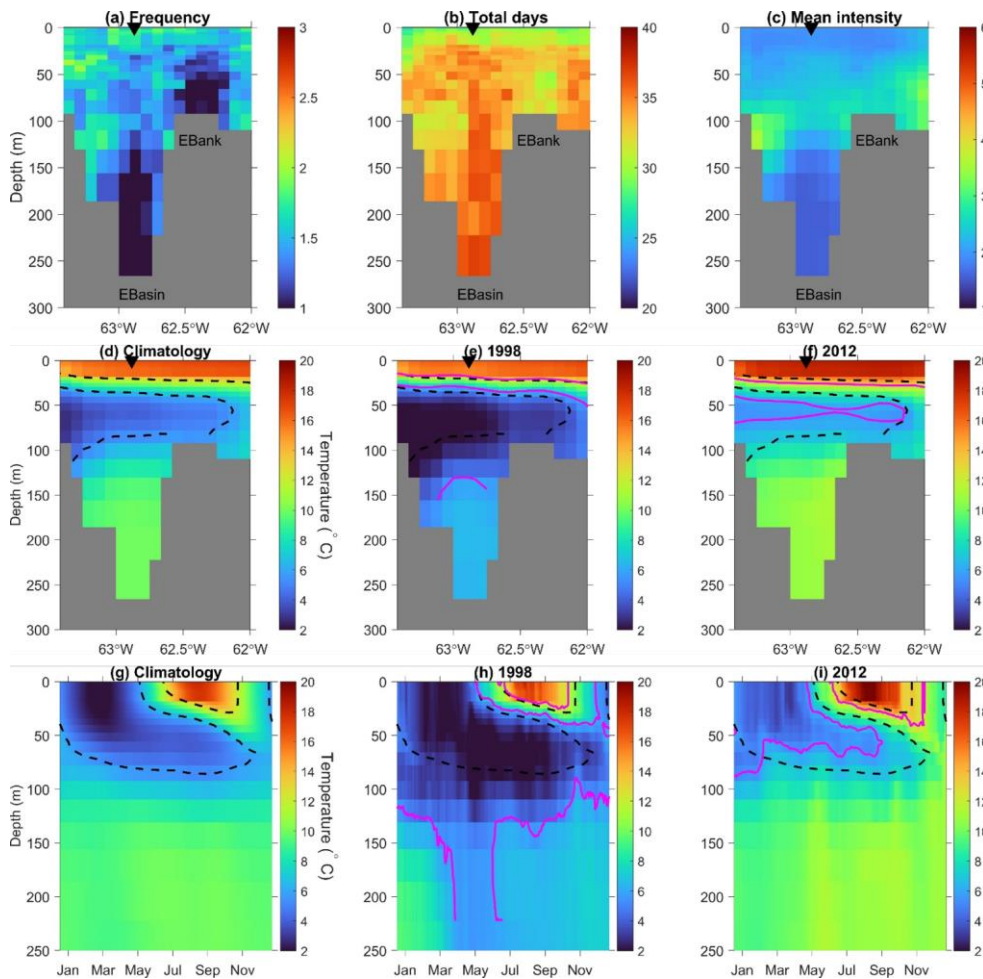


Figure 3: Along the Halifax line (a line between stations 1 and 2 shown in Fig. 1a): (a-e) MHW (a) mean annual frequency (unit in number of events per year), (b) mean of annual total days (unit in days per year), and (c) mean intensity (unit in °C); (d-f) summer (July-September) temperature (d) climatology over 1993-2022, in (e) 1998 and (f) 2012, along the Halifax line, and (g-i) temperature evolution at a station (marked by a black triangle) along the

Halifax line. The station is marked as the solid black triangle in panels a-f). Seasonal evolution of temperature (d-g) climatology averaged over 1993-2022. Temperature in (h) 1998 (e, h) and (i) 2012 (f, i). Contour lines denote the isotherms of 6 and 12 °C. (d-i) dashed black contours for averaged over 1993-2022, and solid magenta contours in (e, h) 1998 and (f, i) 2012, are denoted with black and magenta curves, respectively. Abbreviations: EB_{basin} is Emerald Basin; EB_{bank} is Emerald Bank.

To examine the linkages between surface and water column extreme events, we show the distributions of MHW parameters in the water column along a section extending off the coast from Halifax between stations 1 and 2 (Figs. 3a-c). This cross-section, referred to as the Halifax Line, has been regularly occupied by within the AZMP over multiple decades thus proving extensive observed hydrographic data to assess the quality of. We chose this section because we can compare model-based data such as GLORYS12V1. data with hydrographic observations along this section which are routinely measured by the AZMP monitoring program. Figures 3a-c present the distributions of MHW parameters in the water column along a section extending off the coast from Halifax between stations 1 and 2 (marked in Fig. 1). The MHW mean intensity (Fig. 3c) shows a clear 3-layer structure, with values of about 2°C in the upper layer from surface to a mid-depth interface (decreasing from about 70 m near the coast to about 30 m on the Emerald Bank), high values of 3-3.5°C in the middle layer from the mid-depth interface to about 130 m, and low values of 1.5-2°C below 130 m depth in the Emerald Basin. The annual NHW-MHW frequency (Fig. 3a) is relatively uniform in the water column with values 1.5-2, except low values (<1) below 130 m depth in the Emerald Basin and below 30 m depth over the Emerald Bank where the annual MHW duration is high.

The distribution of MHW parameters in the water column can be explained by the layered structure of temperature along this section in summer (Figs. 3d-f) and the seasonal evolution of the vertical profiles of temperature at a location in the middle of Emerald Basin (Figs. 3g-i), for the mean climatology averaged over 1993-2022, and in the cold and warm years of 1998 and 2012, respectively. The upper layer (from the surface to the mid-depth interface 50 m) shows strong seasonal variations. This layer is well mixed in fall/winter, and has strong stratification developed from spring to summer. Seasonal and interannual variations in this upper layer are mainly due to variations of the surface heat flux, and near the coast are also influenced by the advection of variations in the outflowing waters from the Gulf of St. Lawrence waters with strong seasonal and interannual variations in temperature and salinity which are also mainly driven by the surface flux (Umoh and Thompson, 1994; Dever et al., 2016). The overall major influence of surface heat flux results in a nearly uniform distribution of the MHW parameters in the upper layer. The middle layer (from the mid-depth interface 50 m to about 130 m depth) presents moderate seasonal variations which can be related to the downward penetration of the upper layer surface anomalies driven by surface winds and mixing. On the other hand, this layer is also influenced by the lateral advection of water masses carried by the horizontal currents, mainly from the Cabot Strait subsurface water (30-50 m) and the warm Scotian Slope water and with a smaller portion from the Cabot Strait cold-intermediate layer (50-120 m) and the inshore Labrador Current (Dever et al., 2016). The contributions of the lateral advection vary from the coast to offshore, resulting in the horizontal transition of the depth range of the mid-depth layer getting smaller thinner from near the coast to the Emerald Bank. The influences of surface forcing and horizontal advection cause high MHW intensity across the whole mid-depth layer, and the low MHW frequency over the

Commented [ZL(4)]: Comment from Justine: Can you quantify this with a depth value in meters? (e.g. 50 m, since you are saying that it is well mixed in fall/winter)

Commented [LY(SR4)]: OK

Emerald Bank. The deep layer below 130 m depth in the Emerald Basin (Fig. 3g) presents weak seasonal variations with a near constant temperature of 10°C. However, this layer became colder in 1998 and warmer in 2012 than the climatology (Figs. 3h-i), suggesting ~~but~~ strong interannual variations ~~(Figs. 3g-i) of temperatures in this layer~~. The temperature variations in this deep layer are mainly caused by the intrusion of the offshore water (Dever et al., 2016), leading to low MHW intensity and frequency, and long durations.

3.3 Interannual variations of MHW/MCS parameters

Interannual variations of the MHW/MCS parameters at location 1 in the inner Scotian Shelf are presented in Fig. 4, and some of their statistical quantifications are summarized in Table 2. For the surface parameters (Fig. 4 left columnpanels), variations of their values derived from GLORYS12V1 have high correlations with those derived from CMC-SST except for the MCS mean intensity. The surface MHW (MCS) total days (Figs. 4a and e) show strong interannual variations which have significantly positive (negative) correlations with the annual SST anomalies from GLORYS12V1 (Table 2). The MHW/MCS mean intensities show weaker interannual variations and have no significant correlations with the SST anomalies.

For the bottom parameters (Fig. 4 right columnpanels), significant correlation values derived from GLORYS12V1 and available mooring data are found for the MHW frequency, total days and mean intensity, but not for the MCS parameters (Table 2). This can be attributed to GLORYS12V1 not being able to reproduce the intense cold spikes in the mooring observations data (Fig. 2m). For both the bottom MHWs and MCSs, interannual variations of their frequency, total days and mean intensity all have significant correlations with the annual bottom temperature anomalies from GLORYS12V1. The bottom MHW total days and mean intensity derived from the mooring data are significantly lower than those derived from GLORYS12V1. This is due to the differences in the bottom temperature climatology of the two datasets defined for the calculation of the MHW/MCS parameters. While the two datasets show similar values and increasing trends in the bottom temperatures, the climatology of mooring data during the recent 16 years of 2008-2023 has a higher level averaged temperature than that of GLORYS12V1 during 30 years of 1993-2022 (Fig. 4i). As a result, the mooring data obtains shorter and weaker bottom MHW events than GLORYS12V1. ~~We tested the above hypothesis using the same reference period of 2008-2023. If the same reference period of 2008-2023 is used, the difference in MHW parameters between mooring data and GLORYS12V1 is largely reduced. This suggests e that the calculation of MHW/MCS parameters is strongly impacted by the duration chosen differences in climatology between GLORYS and the mooring data underscore the importance of the baseline chosen for computing the climatology, and whether detrending is applied, as discussed in Capotondi et al. (2024) and Smith et al. (2024).~~

At location 1 during 1993-2023, both at surface and bottom, interannual variations of the MHW and MCS total days are negatively correlated; the intensity and total days of MHWs show positive trends, while those for MCSs show negative trends (Table 2). These correspond to warming trends in both the SST and bottom temperature (Figs. 4i-j). The MHW and MCS mean intensities show no significant trends at surface, but positive trends at bottom (Table 2). For the bottom

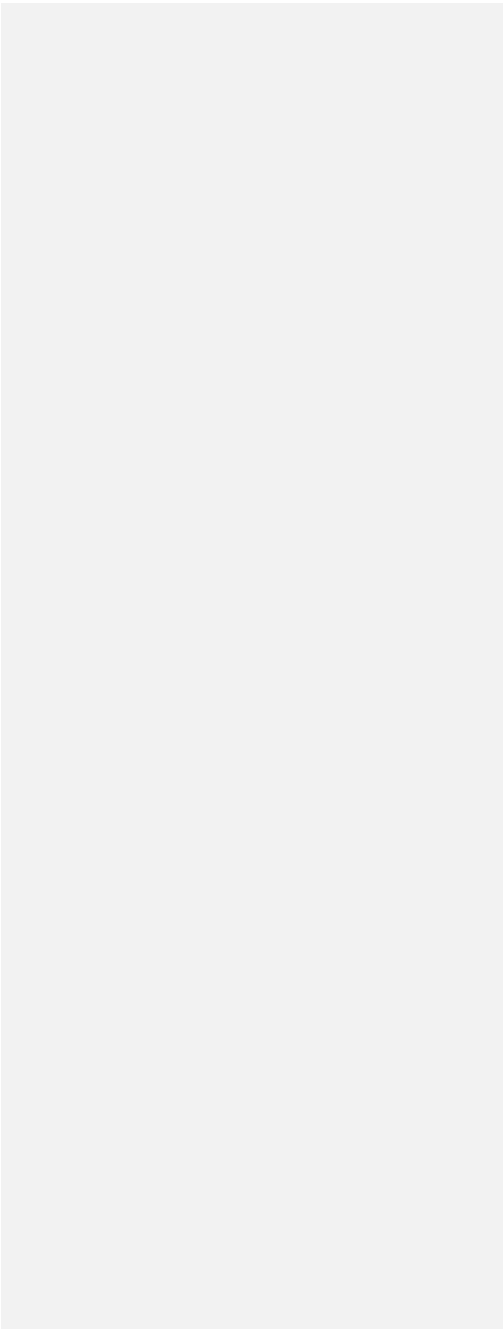
MHW/MCS total days, the trends are mostly due to their sharp increases (or regime shift) around 2012 (Figs. 4b & f). Out of the 19 years before 2012, bottom MCS events are detected in 11 years while MHW events are detected only in 2 years. By comparison, out of the 12 years since 2012, bottom MHW events are detected in 10 years while MCS events are detected only in one year. These correspond to the sharp increase of bottom temperature that also occurred around 2012 (Fig. 4j). By comparison, the SST at location 1 shows a more gradual increasing trend (Fig. 4i). After 2012, the annual bottom temperature became higher than the annual SST. As a result, the bottom MHW total days frequently exceeded 200, higher than 50 for large values of the surface MHW total days (Figs. 4a and b). ~~If we want to use MHW to indicate water mass composition changes, we may need to remove the long-term temperature trends before conducting MHW analysis.~~ The long-term trends and regime shifts of bottom MHW/MCS total days are widespread on the Scotian Shelf, as evidenced by the similar time series as location 1 – at a location in the Emerald Basin and location 7 on the Emerald Shelf (Fig. A2). ~~This raises the question about whether how to define MHWs/MCSs in the presence of long-term trends or regime changes in ocean temperature, a point to be discussed in Section 4.~~

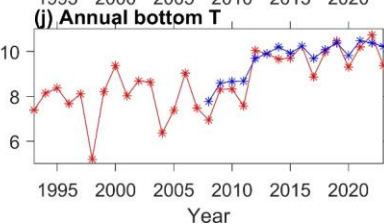
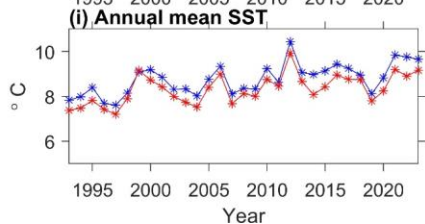
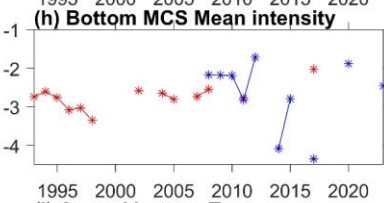
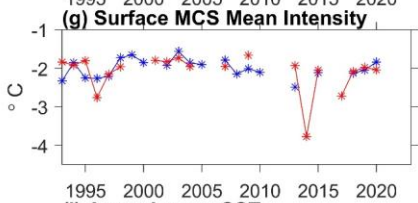
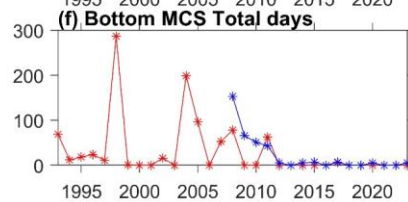
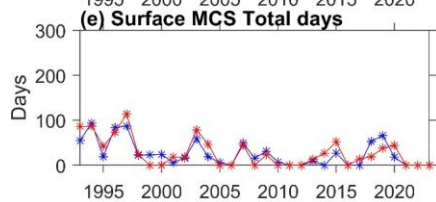
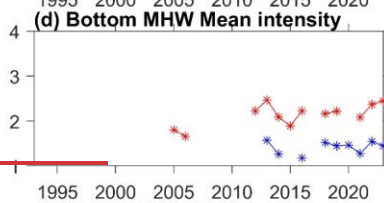
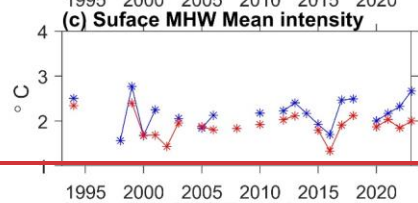
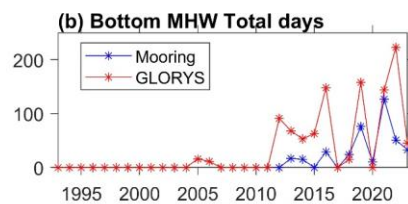
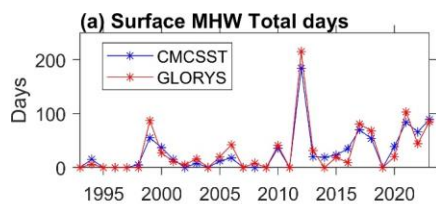
The time series plots identify years when severe MHW or MCS events occurred. At location 1, the surface MHW total days show the highest values in 2012, reaching 215 days according to GLORYS (Fig. 4a). Both GLORYS and CMC-SST detected 7 MHW events and each one lasted with the duration ranging from 7 to 61 days. These prolonged surface MHW events correspond to the highest peak of annual SST (Fig. 4i) and the well-known warming condition across the Scotian Shelf (Hebert et al., 2013) and, in the Gulf of Maine and the east coast of the USA in 2012 (Chen et al., 2015). In December 2011, the SST in the region was close to the 90th percentile and likely played a role in preconditioning the MHW in January 2012. Chen et al. (2015) further attributed the widespread MHW events to persistent atmospheric high-pressure systems featured by anomalously weak wind speeds, increased insolation, and reduced ocean heat losses. At location 1, the termination of a long-lasting and strong surface MHW event in the summer of 2012 (Fig. 3i) can be attributed to wind-induced coastal upwelling, resulting in a sudden drop in SST at the end of August (Shan and Sheng, 2022).

In 2012 at location 1, the bottom MHW total days experienced a sharp increase relative to previous years, reaching ~100 days according to GLORYS (Fig. 4b). In the summer of 2012, the entire water column along the Halifax Line was warmer than the climatology (Figs. 3d and f). In the Emerald Basin (Figs. 3g and i), the abnormally warm condition presented from the surface to about 100 m depth at the beginning of the year (winter), which can be attributed to the smaller heat loss to the atmosphere at the sea surface. Below the 100 m depth, warming started in spring. Below the upper layer directly influenced by surface forcing, the warming in 2012 can be attributed to ~~advection over the Scotian Shelf between 30–50 m, the advection of anomalously warm slope water combined with the reduced contribution of the cold water from the Gulf of St Lawrence or the inner Labrador Shelf between 50–100m, and the anomalously warm slope water being advected onto the shelf between 100–200 m. the advection of abnormally warm Scotian Slope water combined with the reduced contribution of the cold water from the Gulf of St Lawrence or the inner Labrador Shelf~~ (Dever et al., 2016). The warm Scotian Slope water was influenced by the interaction between the Gulf Stream and the Labrador Current at the tail of the Grand Banks of Newfoundland (Brickman et al., 2018; Gonçalves Neto et al., 2023).

The condition in 1998 is opposite to that in 2012, i.e., 1) location 1 experienced the longest bottom MCS total days (nearly 300 days) associated with the lowest annual bottom temperature value (Figs. 4f and e); 2) in summer the entire water column along the Halifax Line was colder than the climatology (Figs. 3d and e); and 3) in the Emerald Basin (Figs. 3g and h) the entire water column was ~~enormously-anomalously~~ cold throughout the year except for close to normal condition in the upper layer in summer. Below 150 m depth in the Emerald Basin, the lowest temperature occurred during March-June. This can be related to the intrusion of the cold Labrador Slope water. According to Drinkwater et al. (2003), this cold water mass was advected along the shelf break in 1997–1998 and flooded the lower layers of the central and southwestern regions of the Scotian Shelf.

In 2023 [at location 1](#), according to GLORYS12V1, the [surface](#) MHW total days is 85 ([Fig. 4a](#)), which is well above the average value of 31 days. The mean intensity ~~was~~ 2°C ([Fig. 4c](#)), similar to the ~~normal-multi-year averaged~~ intensity. The longest [surface](#) MHW event of that year began on December 19, 2022, and continued until February 8, 2023, coinciding with the warmest January on record in Halifax. The termination of this MHW event is likely related to an extremely cold Arctic air outbreak that set many local meteorological records in early February in Atlantic Canada and caused rapid drops of water temperature in some shallow coastal bays (Casey et al., 2024).





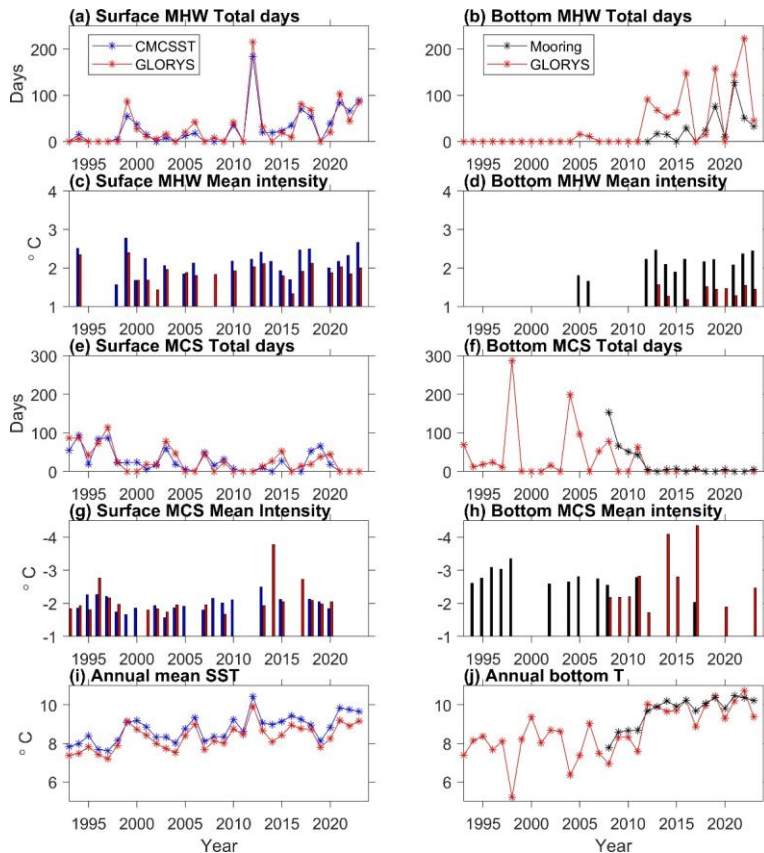


Figure 4: Time series of MHW and MCS characteristics at location 1 (marked in Fig. 1). Left for surface (a, c, e, g and i) and right for bottom (b, d, f, h and j). Row-1: (a, b) MHW total day; (c, d) row-2: MHW mean intensity; row-3: (e, f) MCS total days; row-4: (g, h) MCS intensity; row-5: (i, j) comparison of annual mean time series of GLORYS12V1 with CMC-SST and mooring data observations.

	Trend	Correlation between with obs MHW/MCS from GLORYS12V1 and observations	Correlation between MHW/MCS parameters and with T
Surface			
MHW frequency	0.07 events/yr	0.83	0.8685
MHW total days	1.9 days/yr	0.96	0.81
MHW intensity	-	0.77	-
MCS frequency	-0.1 events/yr	0.69	-0.80
MCS total days	-1.8 days/yr	0.84	-0.81
MCS intensity	-	-	-
Bottom			
MHW frequency	0.2 events/yr	0.770	0.72
MHW total days	4.1 days/yr	0.6975	0.7
MHW intensity	0.03 °C/yr	0.64	0.59
MCS frequency	-0.1 events/yr	-	-0.75
MCS total days	-2.3 days/yr	0.78-	-0.78
MCS intensity	0.03 °C/yr	-	0.59

Table 2: Statistics of annual values of MHW/MCS parameters during 1993-2023 at location 1 on the inner Scotian Shelf. Column 2: linear trends of MHW/MCS frequency in events/year, total days in days/year, and mean intensity in °C/year derived from GLORYS12V1. Column 3: correlation coefficient of MHW/MCS parameters derived from GLORYS12V1 and ~~observed temperature from CMC-SST at the surface and mooring temperature at the sea floor~~. Column 4: correlation coefficient between MHW/MCS parameters and annual GLORYS12V1 temperature. Significant trends and correlations with p-values less than 0.1 are shown.

4 Conclusions and discussions

First, in this study the ~~annual mean MHW~~MHW/MCS parameters derived from GLORYS12V1 and observational data are compared. At ~~the~~ surface, GLORYS12v1 and CMC-SST obtain similar magnitudes, spatial distribution and interannual variations of MHW/MCS frequency, total days and mean intensity. Differences in the values of the parameters can be attributed to issues in the CMC-SST data: 1) shorter MHW total days in the Gulf of St. Lawrence and Labrador ~~and Newfoundland Shelf due to the higher threshold values caused by~~ the missing SST data in the presence of ice, and 2) less frequent MHWs on the deep Scotian Slope associated with weaker SST variations caused by the interpolations and cloud correction applied to the satellite remote sensing data for generating the CMC-SST. Thus, we suggest that ~~high-resolution data assimilative ocean reanalysis products possess-present~~ more advantages in quantifying surface MHWs and MCSs than SST products based on satellite remote sensing. For the bottom MHWs and MCSs, the analysis results from GLORYS12V1 are compared with those from 16 years of bottom mooring observations at location 1 near the coast of Nova Scotia.

Formatted: Indent: First line: 0"

Commented [LZ6]: Justine: Has a similar comparison / conclusion been made for other regions of the ocean?

Commented [LY(7R6)]: Ok for now

GLORYS12V1 captures all parameters of observed bottom MHWs and the total days of bottom MCSs at this location. However GLORYS12V1 does not reproduce the intense cold spikes of observed bottom temperature and hence detects fewer and less intense bottom MCSs at this location. This can be attributed to is likely associated with the weaker variations of the Nova Scotia Current simulated by the spatial resolution GLORYS12V1 that is insufficient to resolve the sharp spatial gradients of the Nova Scotia Current. Therefore near the coast of Nova Scotia, for bottom MCS metrics derived from GLORYS12V1 underestimates the frequency and intensity of the bottom MCSs, although provides estimates of the total days in agreement with the mooring data. we should use the more reliable parameter of total days, and avoid using frequency and intensity. GLORYS does not reproduce the intense cold spikes of observed bottom temperature hence potentially detect less bottom MCSs at this location strongly influenced by the variations of Nova Scotia Current. GLORYS well reproduces the observed rising trend and sharp increase of bottom temperature around 2012 on Scotian Shelf, thus the total days derived from GLORYS are the most reliable parameter to. The 31 years (1993–2023) of GLORYS data enables the quantification of the spatial variations, interannual variations and long-term trends of the water column and bottom MHW/MCS parameters for the first time in our study region.

Second, the horizontal/depth distributions of the annual MHW/MCS parameters are explained by the characteristics of temperature variations and the related ocean dynamics. The corresponding parameters of surface MHWs and MCSs are overall similar due to the nearly symmetrical probability distribution of SST anomalies around the mean, except on the Scotian Slope where the MHWs have lower frequency and higher mean intensity than the MCSs due to the dominance of warm-core eddies. The surface MHWs have the highest frequency (2–3 events per year) and mean intensity (3–6°C) on the Scotian Slope and to the east of southern GBN Grand Banks, due to the strong SST variability associated with the eddy activities and variations of Gulf Stream and North Atlantic Current. The shelf waters show nearly uniform values of the surface MHW parameters: 1–2 events per year for frequency, 20–30 days per year for total days, and ~2.0°C for the mean intensity. The bottom MHW frequency, duration (approximately total days divided by frequency) and mean intensity vary strongly with bottom depth, which can be explained by the layered structure of MHW parameters and temperature along a cross-shelf section off Halifax (Fig. 3). In the upper layer from surface to a mid-depth interface, the nearly uniform MHW mean intensity of ~2°C can be mainly attributed to variations of the surface heat flux. From the mid-depth interface to about 130 m depth, the MHW mean intensity has high values of 3–3.5°C which can be related to the combined effects of downward penetration of the upper layer (through wind forcing and mixing) and the lateral advection of water masses from the Cabot Strait subsurface and cold-intermediate layers, the Scotian Slope water and the inshore Labrador Current. In the deep Emerald Basin below 130 m depth, the MHW intensity has the lowest values of 1.5–2°C due to intrusions of offshore water. The MHW frequency has relatively uniform values of 1.5–2 events per year in the water column, except low values of less than 1 event per year (corresponding to longer MHW durations) below 130 m depth in the Emerald Basin and below 30 m depth over the Emerald Bank. This can be attributed to the different characteristics of temperature variations caused by different forcings: stronger variations at shorter (longer) time scales by surfacing forcing (lateral intrusion).

Commented [LZ8]: Justine: I think this needs an explanation as to why GLORYS doesn't reproduce these -- limited spatial or temporal resolution or something else?

Thirdly, analysis of the GLORYS12V1 data reveals interannual variations, long-term trends and regime shifts of MHW/MCS parameters during 1993-2023. For the surface MHW (MCS) total days, 1) their annual values have significantly positive (negative) correlations with the annual SST anomalies; 2) their increasing (decreasing) trends correspond to the gradual increasing SST; and 3) the peak value (215 days) of MHW total days in 2012 corresponds to the highest annual SST representing the well-known warming condition across the Scotian Shelf, Gulf of Maine and the east coast of the USA. The bottom temperature shows a stronger increasing trend than the SST, and a sharp increase (regime shift) around 2012. This causes the increasing (decreasing) trend and regime shift of MHW (MCS) total days. After 2012 at location 1, the annual bottom temperature became higher than the annual SST; and the bottom MHW total days frequently exceeded 200, higher than 50-70 for large values of the surface MHW total days. At location 1 near the coast of Nova Scotia, GLORYS12V1 well reproduces the rising trend and sharp increase of bottom temperature around 2012 in the mooring data. In 2012, the bottom MHW total days at location 1 experienced a sharp increase to ~100 days. Consistent with the AZMP observations, GLORYS12V1 shows that in 2012 and the entire water column along the Halifax Line was warmer than the climatology, which can be attributed due to the smaller heat loss to the atmosphere at the sea surface, the advection of abnormally warm Scotian Slope water, and the reduced contribution of the cold water from the Gulf of St Lawrence or the inner Labrador Shelf. Opposite conditions ~~presented~~ ~~occured~~ ~~occurred~~ in 1998 with the longest bottom MCS total days of ~300 days at location 1, and the entire water column along the Halifax Line was colder than the climatology. Further studies are needed to link variations of ocean temperature and MHW/MCS parameters in the Northwest Atlantic, at interannual and longer time scales, to large-scale ocean-atmosphere processes. Our study does not attempt to explain what may cause the interannual variability of MHW/MCS characteristics. For example, using long time series of synthetic data, Gregory et al. (2024) ~~recently highlighted~~ ~~examined global connections between El Niño-Southern Oscillations and variations of~~ ~~in~~ ~~MHWs globally~~ ~~event~~, and identified a linkage between La Niña events in the equatorial Pacific and warm conditions in the Northwest Atlantic. ~~however no causal relationship was investigated.~~ Further studies along this line are important for developing predictions of MHWs and MCSs in the future. ~~While an exploration of these connections is beyond the scope of this study, we plan more studies of such nature in the Northwest Atlantic.~~

We note that the detection of MHWs and MCSs and the quantification of their parameters depend on the reference climatology of ocean temperature, ~~in~~ particularly in our study region with evident warming trends over the past several decades. Defining the climatology over 30 years (1993-2022) with the GLORYS data obtains longer total days and stronger intensity for bottom MHWs, compared with using the recent 16 years (2008-2023) of bottom temperature from mooring observations. There are ongoing debates in the literature about whether the long-term trends in ocean temperature should be included or excluded in MHW research (Oliver et al., 2021; Zhang et al., 2024). Recent studies (Amaya et al., 2023b; Capotondi et al., 2024; Smith et al., 2025) proposed-suggested that both approaches could be useful depending on the applications of interest. The long-term warming trends and short-duration extreme events likely cause different physiological and behavioural responses of marine species. In the present study, the long-term warming trend is retained in defining the

492 water temperature climatology and the detection of MHWs and MCSs, while in the future we may ~~consider to exclude the~~
493 ~~trend~~[explore other definitions](#) when investigating the impacts of MHWs and MCSs on marine ecosystems and fisheries.

494 ~~Previous studies have revealed the linkage of the declining North Atlantic right whale population to the significant~~
495 ~~warming in the Gulf of Maine and the western Scotian Shelf over the recent decades (Meyer-Gutbrod et al., 2021), and the~~
496 ~~impacts of the extreme cold (warm) event in 1998 (2012) on certain fishery species. In 1998, shortly after the cold Labrador~~
497 ~~Slope Water replaced the Warm Slope Water, the catches of porbeagle shark and silver hake in the Emerald Basin~~
498 ~~dramatically declined (Drinkwater et al., 2002). In 2012, the anomalously warm bottom water had opposite effects on lobster~~
499 ~~and snow crab fisheries (Mills et al., 2013; Zisserson and Cook, 2017). We plan more studies of such nature in the Northwest~~
500 ~~Atlantic using the GLORYS reanalysis product validated with observational data such as from the AZMP survey.~~

501

502

503 **Data and code availability**

504 The data used in this study are available as described in Table 1. The code used in this study can be accessed via a GitLab
505 repository upon request via email to the corresponding author.

506

507 **Author contribution**

508 LZ and YL led the conceptualization of the study, analysis and writing of the manuscript. HW refined the scripts of data
509 analysis. GG and SVG contributed to the conceptualization of the study, and editing and reviewing the manuscript.

510

511 **Competing interests**

512 The authors declare that they have no conflict of interest.

513

514 **[Disclaimer](#)**

515 [The Copernicus Marine Service offering is regularly updated to ensure it remains at the forefront of user requirements. In](#)
516 [this process, some products may undergo replacement or renaming, leading to the removal of certain product IDs from our](#)
517 [catalogue. If you have any questions or require assistance regarding these modifications, please feel free to reach out to our](#)
518 [user support team for further guidance. They will be able to provide you with the necessary information to address your](#)
519 [concerns and find suitable alternatives, maintaining our commitment to delivering top-quality services.](#)

520

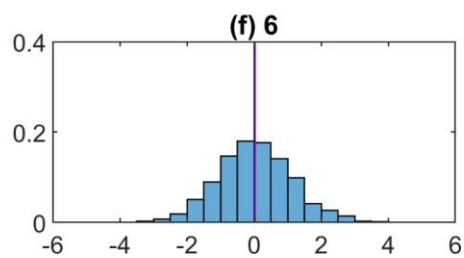
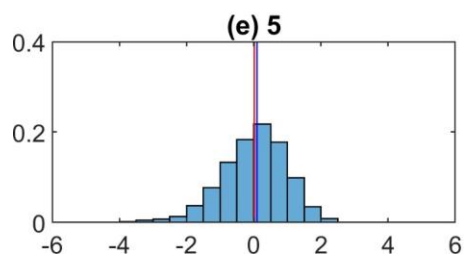
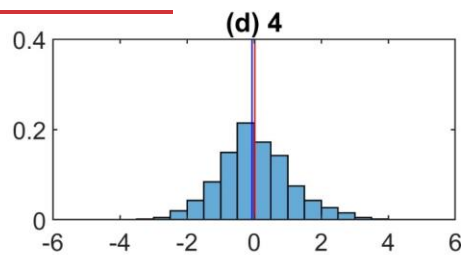
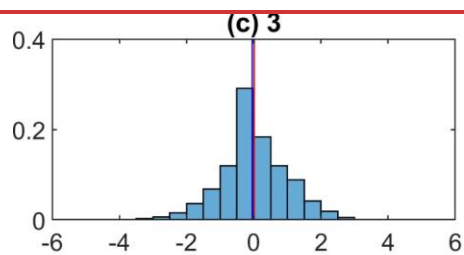
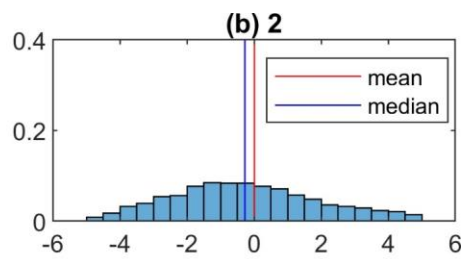
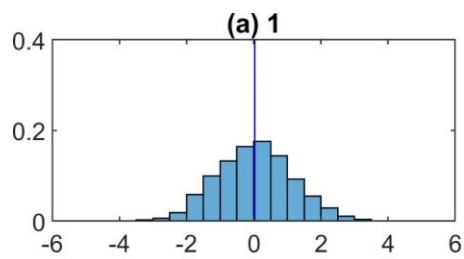
521 [Publisher's note: Copernicus Publications remains neutral with regard to jurisdictional claims in published maps and](#)
522 [institutional affiliations.](#)

523

524 **Acknowledgments**

525 We appreciate DFO and Mercator-Ocean International for supporting the scientific exchanges and collaboration between the
526 staff of both organizations, in recent years under a collaborative agreement, Dr. David Brickman for commenting on an early
527 version of the manuscript, ~~and~~ Dr. Karina Von Schuckmann for insightful comments and advice in developing this
528 manuscript, ~~and Drs. Xianmin Hu, Justine Mcmillan, and Nancy Soontiens for internal reviews, and Dr. Peter Galbraith and~~
529 ~~two anonymous reviewers for detailed, insightful and constructive comments that helped to improve the original manuscript.~~

530
531
532
533
534
535
536



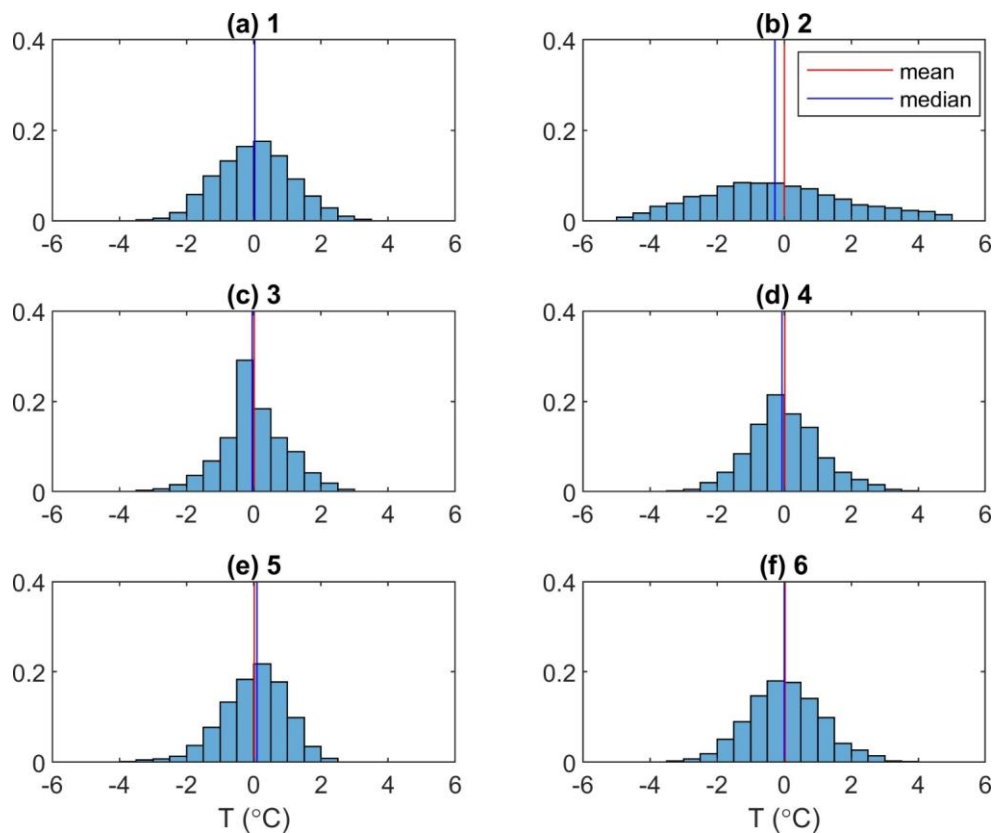


Figure A1: Histogram of sea surface temperature anomalies from GLORYS12V1 at six locations marked in Fig. 1. The height of each bar is the number of observations data values in each bin divided by the total number of observations data values.

Commented [LY(9)]: Is my revision correct?

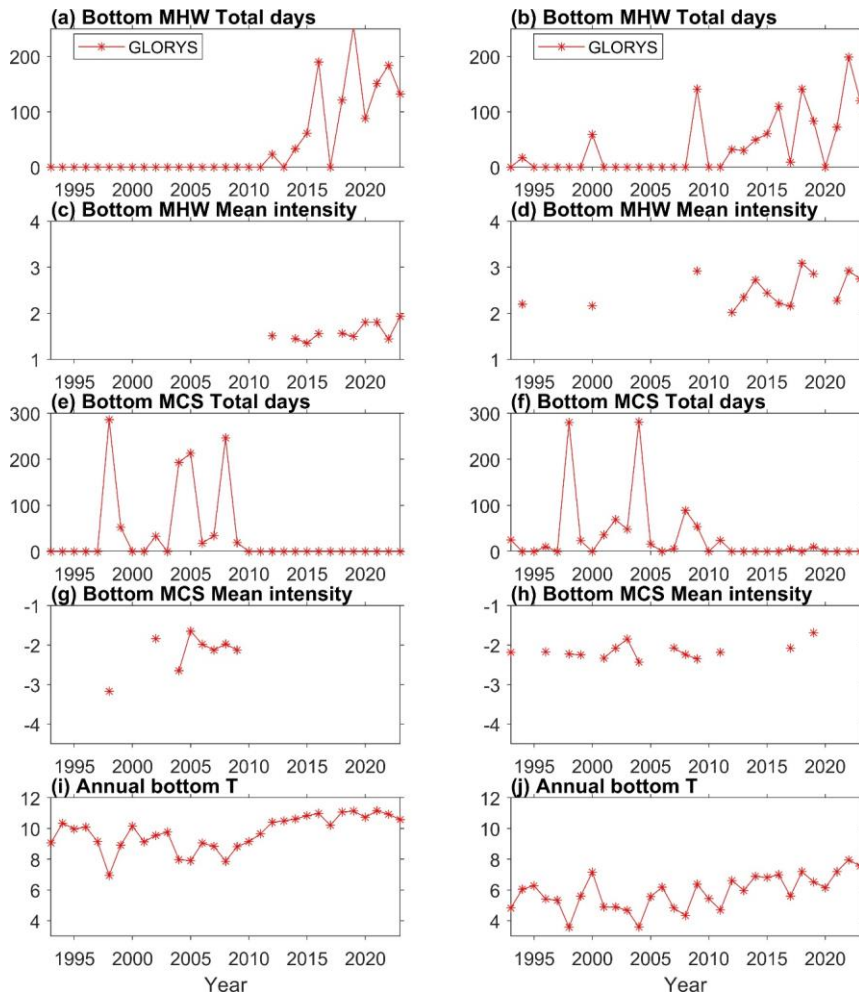


Figure A2. Time series of bottom MHW/MCS ~~paramters~~parameters and bottom temperature derived from GLORYS12V1 at (left column) a location in Emerald Basin (marked as a triangle in Fig. 3a) and (right column) location 7 on Emerald Bank (marked in Figure 1a). ~~The location in Emerald Basin is marked as a triangle in Figure 3a.~~

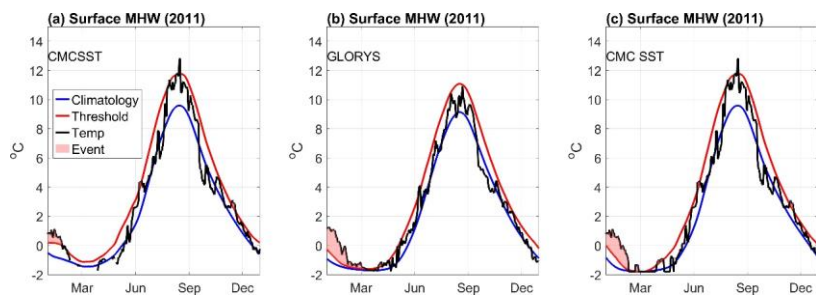


Figure A3. Evolution of surface MHWs in 2011 at a location (52.8°N, 55.2°W) on the Labrador Shelf derived from (a, c) CMC-SST and (b) GLORYS12V1. In (c) the missing values of CMC-SST are filled with the freezing temperature of -1.8 °C.

References:

Amaya, D. J., Jacox, M. G., Alexander, M. A., Scott, J. D., Deser, C., Capotondi, A., and Phillips, A. S.: Bottom marine heatwaves along the continental shelves of North America, *Nat Commun*, 14, 1038, <https://doi.org/10.1038/s41467-023-36567-0>, 2023a.

Amaya, D. J., Jacox, M. G., Fewings, M. R., Saba, V. S., Stuecker, M. F., Rykaczewski, R. R., Ross, A. C., Stock, C. A., Capotondi, A., Petrik, C. M., Bograd, S. J., Alexander, M. A., Cheng, W., Hermann, A. J., Kearney, K. A., and Powell, B. S.: Marine heatwaves need clear definitions so coastal communities can adapt, *Nature*, 616, 29–32, <https://doi.org/10.1038/d41586-023-00924-2>, 2023b.

Beaudin, É., and Bracco, A.: How Marine Heatwaves Impact Life in the Ocean. *Front. Young Minds* 10:712528. doi: 10.3389/frym.2022.712528, 2022.

Brasnett, B.: The impact of satellite retrievals in a global sea - surface - temperature analysis, *Quart J Royal Meteor Soc*, 134, 1745–1760, <https://doi.org/10.1002/qj.319>, 2008.

Brickman, D., Hebert, D., and Wang, Z.: Mechanism for the recent ocean warming events on the Scotian Shelf of eastern Canada, *Continental Shelf Research*, 156, 11–22, <https://doi.org/10.1016/j.csr.2018.01.001>, 2018.

Canada Meteorological Center: CMC 0.2 deg global sea surface temperature analysis. Ver. 2.0. PO.DAAC, CA, USA. Dataset accessed [2023-11-27] at <https://doi.org/10.5067/GHCMC-4FM02>, 2012.

Canada Meteorological Center: GHR SST Level 4 CMC 0.1 deg global sea surface temperature analysis. Ver. 3.0. PO.DAAC, CA, USA. Dataset accessed [2024-03-05] at <https://doi.org/10.5067/GHCMC-4FM03>, 2016.

Capotondi, A., Rodrigues, R.R., Sen Gupta, A., Benthuisen, J.A., Deser, C., Frölicher, T.L., Lovenduski, N.S., Amaya, D.J., Le Grix, N., Xu, T., Hermes, J., Holbrook, N.J., Martinez-Villalobos, C., Masina, S., Roxy, M.K., Schaeffer, A., Schlegel, R.W., Smith, K.E., Wang, C., 2024. A global overview of marine heatwaves in a changing climate. *Commun. Earth Environ.* 5, 1–17. <https://doi.org/10.1038/s43247-024-01806-9>

Gonçalves Neto, A., Palter, J.B., Xu, X., Frantoni, P., 2023. Temporal Variability of the Labrador Current Pathways Around the Tail of the Grand Banks at Intermediate Depths in a High-Resolution Ocean Circulation Model. *J. Geophys. Res. Oceans* 128, e2022JC018756. <https://doi.org/10.1029/2022JC018756>

Smith, K.E., Sen Gupta, A., Amaya, D., Benthuisen, J.A., Burrows, M.T., Capotondi, A., Filbee-Dexter, K., Frölicher, T.L., Hobday, A.J., Holbrook, N.J., Malan, N., Moore, P.J., Oliver, E.C.J., Richaud, B., Salcedo-Castro, J., Smale, D.A., Thomsen, M., Wernberg, T., 2025. Baseline matters: Challenges and implications of different marine heatwave baselines. *Prog. Oceanogr.* 231, 103404. <https://doi.org/10.1016/j.pocean.2024.103404>

Casey, M.P., Petrie, B., Lu, Y., MacDermid, S., and Paquin, JP: Rapid drops of ocean temperatures in several shallow bays in Nova Scotia during a recent cold air outbreak, *Proceedings of the Nova Scotian Institute of Science*, in press, 2024.

Chen, K., Gawarkiewicz, G., Kwon, Y., and Zhang, W. G.: The role of atmospheric forcing versus ocean advection during the extreme warming of the Northeast U.S. continental shelf in 2012, *JGR Oceans*, 120, 4324–4339, <https://doi.org/10.1002/2014JC010547>, 2015.

Collins M., M. Sutherland, L. Bouwer, S.-M. Cheong, T. Frölicher, H. Jacot Des Combes, M. Koll Roxy, I. Losada, K. McInnes, B. Ratter, E. Rivera-Arriaga, R.D. Susanto, D. Swingedouw, and L. Tibig: Extremes, Abrupt Changes and Managing Risk, in: IPCC Special Report on the Ocean and Cryosphere in a Changing Climate, edited by: H.-O. Pörtner, D.C. Roberts, V. Masson-Delmotte, P. Zhai, M. Tignor, E. Poloczanska, K. Mintenbeck, A. Alegría, M. Nicolai, A. Okem, J. Petzold, B. Rama, and N.M. Weyer, Cambridge University Press, Cambridge, UK and New York, NY, USA, 589–655, <https://doi.org/10.1017/9781009157964.003>, 2019.

Dever, M., Hebert, D., Greenan, B. J. W., Sheng, J., and Smith, P. C.: Hydrography and Coastal Circulation along the Halifax Line and the Connections with the Gulf of St. Lawrence, *Atmosphere-Ocean*, 54, 199–217, <https://doi.org/10.1080/07055900.2016.1189397>, 2016.

DFO: 2001 State of the Ocean: Physical Oceanographic Conditions on the Scotian Shelf, Bay of Fundy and Gulf of Maine. DFO Science Ecosystem Status Report 2003/002, 2003.

Drévillon, M., Fernandez, E., Lellouche, J.M.: EU Copernicus Marine Service Product User Manual for the Global Ocean Physics Reanalysis, GLOBAL_MULTIYEAR_PHY_001_030, Issue 1.5, Mercator Ocean International, <https://catalogue.marine.copernicus.eu/documents/PUM/CMEMS-GLO-PUM-001-030.pdf>, last access: 19 March 2024, 2023

Formatted: Font: (Default) +Headings (Times New Roman)

Formatted: Font: (Default) +Headings (Times New Roman), 10 pt

Formatted: Bibliography

Formatted: Font: (Default) +Headings (Times New Roman), 10 pt

Formatted: Bibliography

Formatted: Font: (Default) +Headings (Times New Roman)

Formatted: Font: (Default) +Headings (Times New Roman)

Formatted: French (France)

Formatted: Bibliography

Formatted: Font: (Default) +Headings (Times New Roman), 10 pt

Formatted: Bibliography

Drévilleon, M., Lellouche, J.M., Régnier, C., Garric, G., Bricaud, C., Hernandez, O., and Bourdallé-Badie, R.: EU Copernicus Marine Service Quality Information Document for the Global Ocean Physics Reanalysis, GLOBAL_MULTIYEAR_PHY_001_030, Issue 1.6, Mercator Ocean International, <https://catalogue.marine.copernicus.eu/documents/QUID/CMEMS-GLO-QUID-001-030.pdf>, last access: 19 March 2024, 2023

Drinkwater, K. F., Petrie, B., and Smith, P. C.: Climate variability on the Scotian Shelf during the 1990s, ICES MSS Vol.219 - Hydrobiological variability in the ICES Area, 1990-1999, <https://doi.org/10.17895/ices.pub.19271735.v1>, 2003.

Fiedler, E. K., McLaren, A., Banzon, V., Brasnett, B., Ishizaki, S., Kennedy, J., Rayner, N., Roberts-Jones, J., Corlett, G., Merchant, C. J., and Donlon, C.: Intercomparison of long-term sea surface temperature analyses using the GHR SST Multi-Product Ensemble (GMPE) system, Remote Sensing of Environment, 222, 18–33, <https://doi.org/10.1016/j.rse.2018.12.015>, 2019.

Fox-Kemper, B., Hewitt, H. T., Xiao, C., Aðalgeirsdóttir, G., Drijfhout, S. S., Edwards, T. L., Golledge, N. R., Hemer, M., Kopp, R. E., Krinner, G., Mix, A., Notz, D., Nowicki, S., Nurhati, I. S., Ruiz, L., Sallée, J.-B., Slangen, A. B. A., and Yu, Y.: Ocean, Cryosphere and Sea Level Change, edited by: Masson-Delmotte, V., Zhai, P., Pirani, A., Connors, S. L., Péan, C., Berger, S., Caud, N., Chen, Y., Goldfarb, L., Gomis, M. I., Huang, M., Leitzell, K., Lonnoy, E., Matthews, J. B. R., Maycock, T. K., Waterfield, T., Yelekçi, O., Yu, R., and Zhou, B., Climate Change 2021: The Physical Science Basis. Contribution of Working Group I to the Sixth Assessment Report of the Intergovernmental Panel on Climate Change, 1211–1362, <https://doi.org/10.1017/9781009157896.011>, 2021.

Free, C. M., Anderson, S. C., Hellmers, E. A., Muhling, B. A., Navarro, M. O., Richerson, K., Rogers, L. A., Satterthwaite, W. H., Thompson, A. R., Burt, J. M., Gaines, S. D., Marshall, K. N., White, J. W., and Bellquist, L. F.: Impact of the 2014–2016 marine heatwave on US and Canada West Coast fisheries: Surprises and lessons from key case studies, Fish and Fisheries, 24, 652–674, <https://doi.org/10.1111/faf.12753>, 2023.

Frölicher, T. L., Fischer, E. M., and Gruber, N.: Marine heatwaves under global warming, Nature, 560, 360–364, <https://doi.org/10.1038/s41586-018-0383-9>, 2018.

Galbraith, P. S., Chassé, J., Shaw, J.-L., Dumas, J., and Bourassa, M.-N.: Physical oceanographic conditions in the Gulf of St. Lawrence during 2023, Can. Tech. Rep. Hydrogr. Ocean Sci. 378 : v + 91 p.

Hebert, D., Pettipas, R., Brickman, D., and Dever, M.: Meteorological, Sea Ice and Physical Oceanographic Conditions on the Scotian Shelf and in the Gulf of Maine during 2012, DFO Can. Sci. Advis. Sec. Res. Doc. 2013/058. v + 46 p, 2013.

Hebert, D., Layton, C., Brickman, D., and Galbraith, P. S.: Physical Oceanographic Conditions on the Scotian Shelf and in the Gulf of Maine during 2022, Can. Tech. Rep. Hydrogr. Ocean Sci. 359, vi + 81 p., 2023.2012.

Hobday, A. J., Alexander, L. V., Perkins, S. E., Smale, D. A., Straub, S. C., Oliver, E. C. J., Benthuyssen, J. A., Burrows, M. T., Donat, M. G., Feng, M., Holbrook, N. J., Moore, P. J., Scannell, H. A., Sen Gupta, A., and Wernberg, T.: A hierarchical approach to defining marine heatwaves, Progress in Oceanography, 141, 227–238, <https://doi.org/10.1016/j.pocean.2015.12.014>, 2016.

Holbrook, N. J., Scannell, H. A., Sen Gupta, A., Benthuyssen, J. A., Feng, M., Oliver, E. C. J., Alexander, L. V., Burrows, M. T., Donat, M. G., Hobday, A. J., Moore, P. J., Perkins-Kirkpatrick, S. E., Smale, D. A., Straub, S. C., and Wernberg, T.: A global assessment of marine heatwaves and their drivers, Nat Commun, 10, 2624, <https://doi.org/10.1038/s41467-019-10206-z>, 2019.

Korus, J., Filgueira, R., and Grant, J.: Influence of temperature on the behaviour and physiology of Atlantic salmon (*Salmo Salar*) on a commercial farm, Aquaculture, 589, 740978, <https://doi.org/10.1016/j.aquaculture.2024.740978>, 2024.

Loder, J.W., Petrie, B. and Gawarkiewicz, G.: The coastal ocean off northeastern North America: a large-scale view. Ch. 5 In: The Global Coastal Ocean: Regional Studies and Synthesis. The Sea, Vol. 11, A.R. Robinson and K.H. Brink (eds.), John Wiley & Sons, Inc., p. 105-133, 1998.

Lu, Y., Wright, D. G., and Clarke, R. A.: Modelling deep seasonal temperature changes in the Labrador Sea, Geophysical Research Letters, 33, <https://doi.org/10.1029/2006GL027692>, 2006.

Ma, Y., Lu, Y., Hu, X., Gilbert, D., Socolofsky, S. A., and Boufadel, M.: Model simulated freshwater transport along the Labrador current east of the Grand Banks of Newfoundland, Front. Mar. Sci., 9, <https://doi.org/10.3389/fmars.2022.908306>, 2022.

Formatted: Font: (Default) +Headings (Times New Roman), 10 pt

Formatted: Font: (Default) +Headings (Times New Roman)

Formatted: Font: (Default) +Headings (Times New Roman), 10 pt

Formatted: Font: (Default) +Headings (Times New Roman)

Formatted: Font: (Default) +Headings (Times New Roman), 10 pt

Formatted: Bibliography

Formatted: Font: (Default) +Headings (Times New Roman), 10 pt

Meissner, T., Wentz, F. J., Scott, J., and Vazquez-Cuervo, J.: Sensitivity of Ocean Surface Salinity Measurements From Spaceborne L-Band Radiometers to Ancillary Sea Surface Temperature, *IEEE Trans. Geosci. Remote Sensing*, 54, 7105–7111, <https://doi.org/10.1109/TGRS.2016.2596100>, 2016.

Meyer-Gutbrod, E. L., Greene, C. H., Davies, K. T. A., and Johns, D. G.: Ocean Regime Shift is Driving Collapse of the North Atlantic Right Whale Population | *Oceanography*, n.d.

Mills, K., Pershing, A., Brown, C., Chen, Y., Chiang, F.-S., Holland, D., Lehuta, S., Nye, J., Sun, J., Thomas, A., and Wahle, R.: Fisheries Management in a Changing Climate: Lessons From the 2012 Ocean Heat Wave in the Northwest Atlantic, *oceanog*, 26, <https://doi.org/10.5670/oceanog.2013.27>, 2013.

Mohamed, B., Barth, A., and Alvera-Azcárate, A.: Extreme marine heatwaves and cold-spells events in the Southern North Sea: classifications, patterns, and trends, *Front. Mar. Sci.*, 10, <https://doi.org/10.3389/fmars.2023.1258117>, 2023.

Oliver, E. C. J., Donat, M. G., Burrows, M. T., Moore, P. J., Smale, D. A., Alexander, L. V., Benthuyssen, J. A., Feng, M., Sen Gupta, A., Hobday, A. J., Holbrook, N. J., Perkins-Kirkpatrick, S. E., Scannell, H. A., Straub, S. C., and Wernberg, T.: Longer and more frequent marine heatwaves over the past century, *Nat Commun*, 9, 1324, <https://doi.org/10.1038/s41467-018-03732-9>, 2018.

Oliver, E. C. J., Benthuyssen, J. A., Darmaraki, S., Donat, M. G., Hobday, A. J., Holbrook, N. J., Schlegel, R. W., and Sen Gupta, A.: Marine Heatwaves, *Annual Review of Marine Science*, 13, 313–342, <https://doi.org/10.1146/annurev-marine-032720-095144>, 2021.

Peal, R., Worsfold, M., and Good, S.: Comparing global trends in marine cold spells and marine heatwaves using reprocessed satellite data, *State of the Planet*, 1–osr7, 1–10, <https://doi.org/10.5194/sp-1-osr7-3-2023>, 2023.

Santora, J. A., Mantua, N. J., Schroeder, I. D., Field, J. C., Hazen, E. L., Bograd, S. J., Sydeman, W. J., Wells, B. K., Calambokidis, J., Saez, L., Lawson, D., and Forney, K. A.: Habitat compression and ecosystem shifts as potential links between marine heatwave and record whale entanglements, *Nat Commun*, 11, 536, <https://doi.org/10.1038/s41467-019-14215-w>, 2020.

Schlegel, R. W., Oliver, E. C. J., Wernberg, T., and Smit, A. J.: Nearshore and offshore co-occurrence of marine heatwaves and cold-spells, *Progress in Oceanography*, 151, 189–205, <https://doi.org/10.1016/j.pocean.2017.01.004>, 2017.

Schlegel, R. W., Oliver, E. C. J., and Chen, K.: Drivers of Marine Heatwaves in the Northwest Atlantic: The Role of Air–Sea Interaction During Onset and Decline, *Front. Mar. Sci.*, 8, 627970, <https://doi.org/10.3389/fmars.2021.627970>, 2021a.

Schlegel, R. W., Darmaraki, S., Benthuyssen, J. A., Filbee-Dexter, K., and Oliver, E. C. J.: Marine cold-spells, *Progress in Oceanography*, 198, 102684, <https://doi.org/10.1016/j.pocean.2021.102684>, 2021b.

Sen Gupta, A., Thomsen, M., Benthuyssen, J. A., Hobday, A. J., Oliver, E., Alexander, L. V., Burrows, M. T., Donat, M. G., Feng, M., Holbrook, N. J., Perkins-Kirkpatrick, S., Moore, P. J., Rodrigues, R. R., Scannell, H. A., Taschetto, A. S., Ummenhofer, C. C., Wernberg, T., and Smale, D. A.: Drivers and impacts of the most extreme marine heatwave events, *Sci Rep*, 10, 19359, <https://doi.org/10.1038/s41598-020-75445-3>, 2020.

Shan, S. and Sheng, J.: Numerical Study of Topographic Effects on Wind-Driven Coastal Upwelling on the Scotian Shelf, *Journal of Marine Science and Engineering*, 10, 497, <https://doi.org/10.3390/jmse10040497>, 2022.

Smith, K. E., Sen Gupta, A., Amaya, D., Benthuyssen, J. A., Burrows, M. T., Capotondi, A., Filbee-Dexter, K., Frölicher, T. L., Hobday, A. J., Holbrook, N. J., Malan, N., Moore, P. J., Oliver, E. C. J., Richaud, B., Salcedo-Castro, J., Smale, D. A., Thomsen, M., and Wernberg, T.: Baseline matters: Challenges and implications of different marine heatwave baselines, *Progress in Oceanography*, 231, 103404, <https://doi.org/10.1016/j.pocean.2024.103404>, 2025.

Soontiens, N., Andres, H. J., Coyne, J., Cyr, F., Galbraith, P. S., Penney, J.: An analysis of the 2023 summer and fall marine heat waves on the Newfoundland and Labrador Shelf: the impact of stratification, winds, and advection, *Oceans State Report* 9, 20254.

Thompson, K. R. and Demirov, E.: Skewness of sea level variability of the world’s oceans, *Journal of Geophysical Research: Oceans*, 111, <https://doi.org/10.1029/2004JC002839>, 2006.

Umoh, J. U. and Thompson, K. R.: Surface heat flux, horizontal advection, and the seasonal evolution of water temperature on the Scotian Shelf, *Journal of Geophysical Research: Oceans*, 99, 20403–20416, <https://doi.org/10.1029/94JC01620>, 1994.

Wang, H., Lu, Y., Zhai, L., Chen, X., and Liu, S.: Variations of surface marine heatwaves in the Northwest Pacific during 1993–2019, *Front. Mar. Sci.*, 11, 1323702, <https://doi.org/10.3389/fmars.2024.1323702>, 2024.

Formatted: Font: (Default) Times New Roman, 10 pt

Formatted: Font: (Default) +Headings (Times New Roman), 10 pt

Formatted: Indent: Left: 0", Hanging: 0.5"

702 Wang, Y., Kajtar, J. B., Alexander, L. V., Pilo, G. S., and Holbrook, N. J.: Understanding the Changing Nature of Marine
703 Cold-Spells, *Geophysical Research Letters*, 49, e2021GL097002, <https://doi.org/10.1029/2021GL097002>, 2022.
704 Zhang, M., Cheng, Y., Wang, G., Shu, Q., Zhao, C., Zhang, Y., and Qiao, F.: Long-term ocean temperature trend and marine
705 heatwaves, *J. Ocean. Limnol.*, <https://doi.org/10.1007/s00343-023-3160-z>, 2024.
706 Zhao, Z. and Marin, M.: A MATLAB toolbox to detect and analyze marine heatwaves, *Journal of Open Source Software*, 4,
707 1124, <https://doi.org/10.21105/joss.01124>, 2019.
708 Zisserson, B. and Cook, A.: Impact of bottom water temperature change on the southernmost snow crab fishery in the
709 Atlantic Ocean, *Fisheries Research*, 195, 12–18, <https://doi.org/10.1016/j.fishres.2017.06.009>, 2017.

Formatted: Font: (Default) +Headings (Times New Roman)